



Fabrication and electrical characterization of $(\text{Bi}_{0.49}\text{Na}_{0.49}\text{Ba}_{0.02})\text{TiO}_3$ -PVDF thin film composites

Sugato Hajra¹ · Sushrisangita Sahoo² · R. N. P. Choudhary²

Received: 8 July 2018 / Accepted: 5 December 2018 / Published online: 12 December 2018
© The Polymer Society, Taipei 2018

Abstract

The barium doped bismuth sodium titanate (i.e., $\text{Bi}_{0.49}\text{Na}_{0.49}\text{Ba}_{0.02}\text{TiO}_3$ (BNBT) powder was prepared by a conventional ceramic processing route. The thin film composites of BNBT- PVDF (polyvinylidene fluoride) were fabricated via a solution casting route. The scanning electron micrographs of the thin film samples show the homogenous distribution of grains with absence of cracks/pores. It is observed that with the increase of BNBT content in PVDF leads to enhancement in the dielectric permittivity and the reduction in the dissipation factor (tangent loss). The various electrical properties of the thin film samples were studied in the frequency range of 1 kHz to 1 MHz at different temperature between 25 and 100 °C. The prepared composite films have been used to study the (a) relationship between properties and crystal structure and (b) relaxation and conduction mechanism through the complex modulus and impedance spectroscopy. The contribution of grains was analyzed in the composite films by the fitting of equivalent circuit with the experimental data. An existence of the non-Debye type of dielectric relaxation was indicated by studying of the impedance and modulus parameters. The calculated activation energy from the temperature dependence of AC conductivity depicts hopping nature of charge carriers, which further explain the conduction process and mechanism in the prepared composites.

Keywords Ceramic-polymer composites · Dielectric · Impedance spectroscopy

Introduction

For the past few decades, the ceramic-polymer composites are considered as a new family of functional materials that are of a great research and technological interest. The excellent properties exhibited by such composites are high permittivity, low tangent loss, high energy storage density, high breakdown strength, flexibility and low density. They have a huge potential for applications in device engineering, such as, gate dielectrics, sensors, electro-optic as well as semiconductor applications [1]. For last few decades, lead zirconate titanate (PZT) and its composites with polymers have widely been used for many sensor applications. Due to the global

environment problems, lead based electronic materials are eliminated for their future use because of the high toxicity of PbO. Several research groups have attempted to find out an alternative to lead based ferroelectric ceramics or polymers and $\text{Pb}(\text{Zr,Ti})\text{O}_3$ ceramics. Further, an alternative tool to eradicate the effect of lead based devices is attempted by the ceramic-polymer composite films. However, the ceramics generally are brittle, low dielectric breakdown and difficulty in processing despite of high permittivity. The ferroelectric ceramics require high processing temperatures, and also have high acoustic impedance which fail to match with human body or water. On the other part, the polymer matrix exhibits high dielectric strength, cheap processing, excellent mechanical properties (flexibility), but permittivity is very low usually 10 [2]. The choice of polymer as a matrix depends on certain factors like economy, physical and thermal properties. So the combination of both ferroelectric ceramic (filler) and polymer (matrix) makes a novel composite with small volume or dimension, high permittivity and capacitance [3]. PVDF is very flexible ferroelectric bearing the highest piezoelectric coefficient, and it does not get depolarize under application of high electric field due to its stability over long period [4]. PVDF

✉ Sugato Hajra
sugatofl@outlook.com

¹ Department of Electronics and Instrumentation, Siksha O Anusandhan (deemed to be university), Bhubaneswar 751030, India

² Multifunctional and Advance Materials Laboratory, Siksha O Anusandhan (deemed to be university), Bhubaneswar 751030, India

consists of four types of phases which are commonly known as δ , β , λ , α having a stereo-chemical representation TGTG⁻, TTTT, TGTG⁻ (polar), T₃GT₃G⁻ (T = trans, G = gauche+, G⁻ = gauche-) [5]. The monomer unit of PVDF is CH₂-CF₂. It has been noticed that after several years of preservation, PVDF remains ferroelectrically stable [6]. In PVDF, due to the stabilization of polar electroactive phase, the problem arises during the batch production of such films in industry hampering its usage in devices. There are several materials (i.e ZnO, BaTiO₃, GaN, ZnSO₃, PZT, BNT based materials) widely used for its superior features, such as energy conversion, but bars its usability as they are brittle and cost intensive and some are toxic. Some of the common applications of such polymer-ceramic composites can be triboelectric based materials [7]. The polymer-ceramic composites are an alternative approach to produce desirable open circuit voltages and can transform mechanical vibration into electrical energy due to its high stability, low density and flexibility. The concept of device miniaturization is common practice by all leading electronics industry lead the cast of processing the low loss high permittivity dielectric materials [8].

Recently, scientific groups put their insight on PVDF due to its better heat stability, high dielectric breakdown strength and easy processing [9]. It is a semi-crystalline and non-toxic polymer that crystallizes in four different forms depending on conditions of annealing, solvent properties and casting method [10]. The ferroelectric nature of PVDF is confirmed from a desirable β - phase. As a result, it is mostly preferred to develop PVDF based dielectric composites. Kobayashi et al. prepared BaTiO₃-PVDF-Siloxane modified polyamideimide and reported four times larger permittivity than that of pure PVDF, large capacitance density of 0.63 nF mm⁻² [11]. Song et al. studied the effect of coupling agent on dielectric parameters of (BaSr)TiO₃/PVDF composite [12]. Thomas et al. reported CaCu₃Ti₄O₁₂/PVDF nano-composite films with high permittivity (≈ 90 at 100 Hz) by combining solution casting and spin coating techniques [13]. Luo et al. reported the structural, microstructural and dielectric properties of BCZT@dopamine/PVDF composite films [14]. Tiwari et al. reported the PVDF/Pb(ZrTi)O₃ composites prepared by solvent casting route and highlighted its dielectric and piezoelectric properties [15].

Due to the multifunctionality of passive components (capacitor) in electronics, its development is of great interest. The main motivation behind this work is to add the external filler in the matrix (PVDF). It is expected that this addition will improve the functionalities of matrix as well as stabilize the γ/β - polymer phases which are very important for the enhancement of the physical properties of the PVDF based ceramic composites. After an extensive survey of reported works, it is discerned that there is no clear and consistent results to understand the relaxation mechanism

and electrical properties of BNBT-PVDF composites. In this communication, the studies of phase purity, morphology, electrical properties (resistive, conducting and insulating) of prepared ceramic-polymer composites in which ceramic phase is randomly spread in particulate form are reported. The loss tangent, the imaginary part of modulus and impedance are correlated because they suggest the different relaxation mechanism in the sample. A further attempt has been made to study the AC conductivity of the prepared composites by complex impedance spectroscopy.

Experimental procedures

Preparation of composites

The fine powder of BNBT was synthesized by a cost effective ceramic processing route. The high-purity or analytical grade oxides and carbonates (i.e., Bi₂O₃ (Central drug house (P) LTD), BaCO₃ (Central drug house (P) LTD), Na₂CO₃ (Central drug house (P) LTD), TiO₂ (Loba Chemie) in stoichiometric ratios were thoroughly mixed in an agate mortar. Next, the homogeneous mixture of the above ingredients was heat-treated for 4 h at 850 °C, and compound formation is confirmed from X-ray structural analysis. The BNBT-PVDF composite films were fabricated of different compositions, such as, 0.1BNBT-0.9PVDF (BP-1), 0.3BNBT-0.7PVDF (BP-2), 0.5BNBT-0.5PVDF (BP-3) using a solution casting route. The PVDF (M/S Himedia, density-1.78 g cm⁻³) acts as polymer matrix while the BNBT served as the filler element. The polymer matrix was first dissolved in DMF (N,N-Dimethylformamide) solvent and stirring was continued for 1 h at 60 °C until the solutions became clear and transparent. Further, the filler element was introduced in the solvent and the mixture was allowed to stir at 60 °C for 30 h. After that the solvent was further heated at 80 °C to allow the evaporation and to achieve concentrated suspensions. Finally, the suspension was cast/poured into casting plate and the film were obtained. The film was placed in an oven for 3 h at 60 °C to eliminate the left out solvent. To get flexibility in the films of various dimensions, a restriction towards the filler loading was taken maximum up to 50 vol%. The films may become brittle if the ceramic loading in the polymer composite exceeds 50 vol%.

Characterization

The X-ray diffraction (XRD) spectra of all the prepared composites were collected employing X-ray powder diffractometer (Rigaku, SmartLab) at room temperature using CuK α radiation ($\lambda = 1.5405 \text{ \AA}$, scan speed = 3 degrees/min). The scanning electron microscope (SEM: FEI Inspect S50, Sweden)

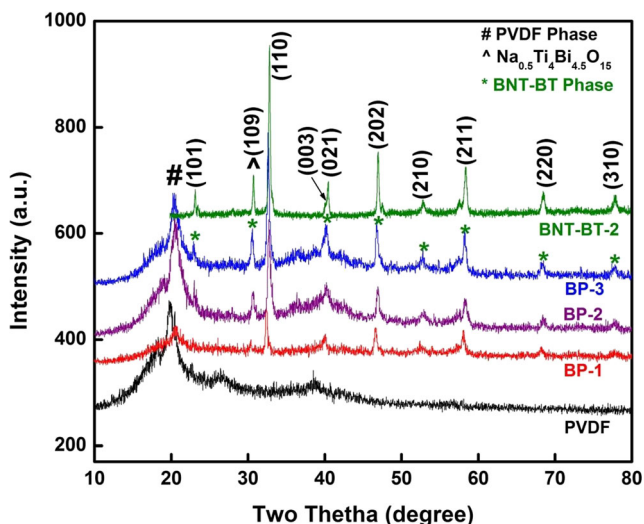


Fig. 1 XRD patterns of Pure PVDF, Pure BNT-BT powder and PVDF/BNT-BT composites (BP-1, BP-2, BP-3)

helps to confirm the fabrication of highly dense composite films and the morphology. For all the electrical measurements (i.e., dielectric, impedance, conductivity) silver paint was painted on both the sides of films. Further, to make it moisture free, it was dried at 140 °C for 1 h. Impedance spectroscopic analyzer (M/S PSM 1735, N4L, UK) provides the data of electrical properties from 1 kHz to 1 MHz frequency range as a function of temperature.

Results and discussion

Structural and morphological analysis

Figure 1 presents the XRD spectra of pure PVDF and the PVDF/BNBT composite films at room temperature. The strong peaks observed at two theta corresponded to 22° (101), 31° (110), 39° (021), 45° (202), 56° (211), 69° (220), 78° (310) represent the BNBT phase with hexagonal perovskite structure. A small impurity peak observed at 31° is assigned to tetragonal phase (ICDD: 04–010-5863). There are three to four crystalline phases of PVDF (i.e., α -, β -, γ - phases) depending upon the processing/ preparation route, such as casting procedure, solvent, temperature of the melt, stretching of composite films. As per the reported data earlier, the characteristic peaks observed are consistent with pure PVDF [16, 17]. The small impurity peak is also seen in the prepared composites (BP-1, BP-2, BP-3) in between range 30°–35°. In the figure, it can be seen, as expected, the perovskite peak got enhanced with the addition of BNBT into the PVDF. The least squares latticed parameters of BNBT are noted as: $a = b = 5.4867 \text{ \AA}$, $c = 6.7155 \text{ \AA}$, $c/a = 1.22$ which is consistent with our previous work [18]. The spectra also reveal that there is no change in the position of the peak or peak shift. This suggests that the variation of BNBT with PVDF shows the same structure in all the prepared composites.

Fig. 2 SEM images of PVDF and BNT-BT/PVDF (BP-1, BP-2, BP-3) composite films

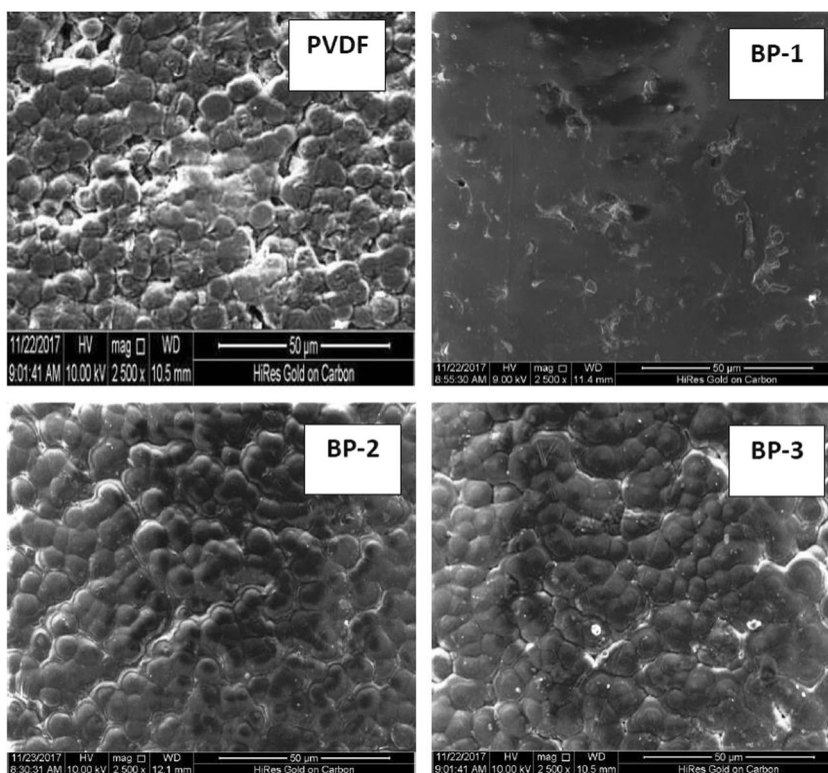


Figure 2 illustrates the morphology and the texture of the composite films employing the scanning electron microscope (SEM). Figure 2 shows neat and clear PVDF film without any

trace of impurities or pores. It also shows the SEM micrograph of composite films BP-1, BP-2, BP-3. Though the grain growth is not uniform, it confirms high density packing in case of

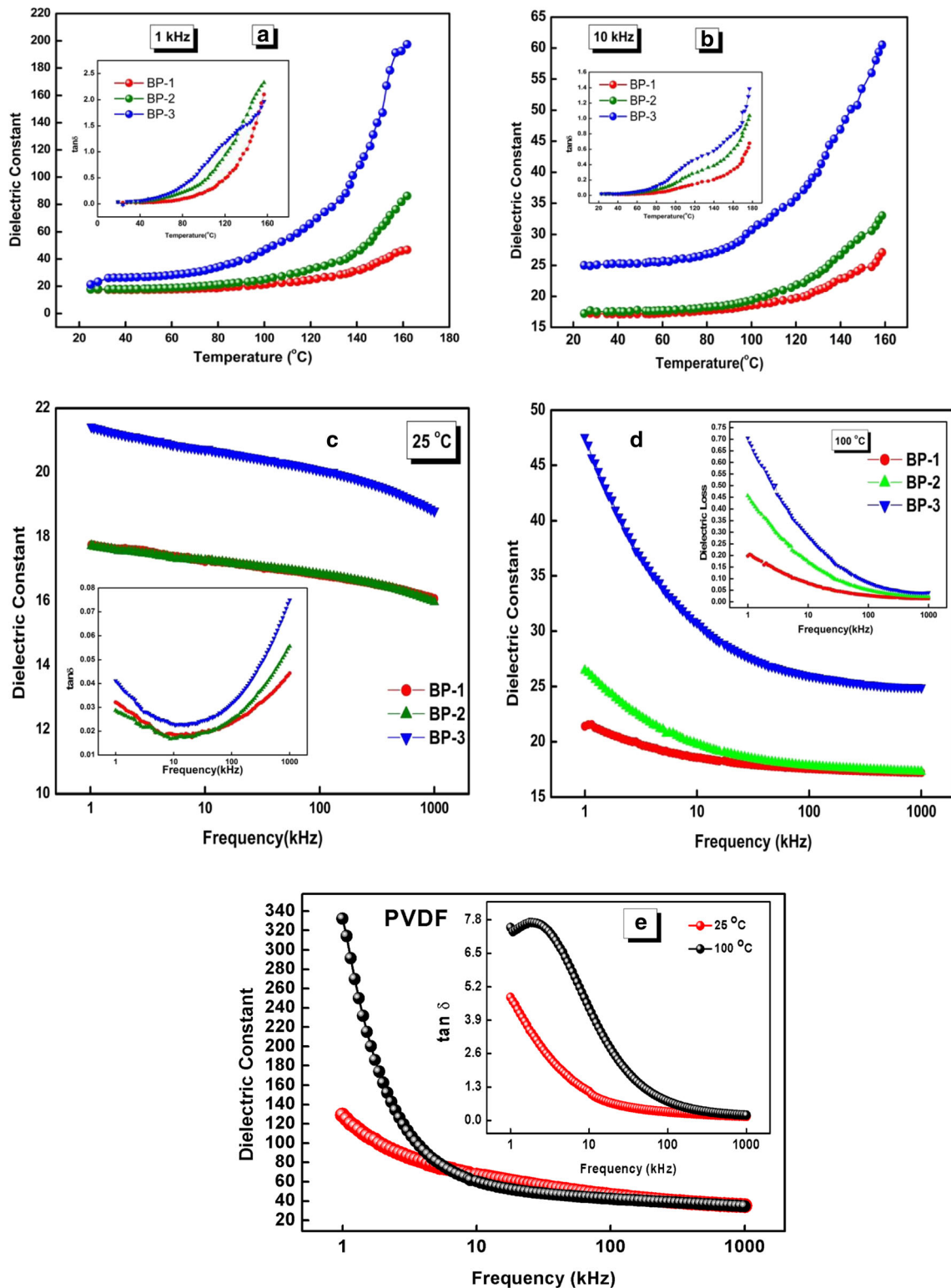


Fig. 3 a, b Temperature dependent dielectric permittivity and loss (inset) at 1 kHz and 10 kHz. Frequency dependent dielectric permittivity and loss (inset) at selected temperature (c) 25 °C and (d) 100 °C. e Frequency dependent dielectric constant and loss factor for PVDF at 25 °C and 100 °C

BNT-BT-2 [18]. The PVDF matrix was seen with inorganic powders over it (particle size: 200–250 nm). The packing or grain growth is denser as the filler content rises suggesting an excellent compatibility between the PVDF and functionalized particles (BNBT). The SEM micrographs suggest that the distribution of particles over PVDF matrix is homogenous throughout, however, some agglomeration of particles is observed.

Dielectric analysis

Figure 3a, b presents temperature dependent dielectric permittivity and tangent loss (inset) in the frequency range of 1 kHz and 10 kHz. It is seen that with an increase in temperature the dielectric constant rises for both the plots. The space charge polarization or diffusion of ions taking place with temperature rise may be the reason of such trend [19]. Additionally, the increased value of permittivity at high temperatures may be due to the thermal energy overcoming the activation barrier of polar molecule arrangement in the direction of the field. The temperature dependent dielectric loss exhibits the same trend as of dielectric constant at both 1 kHz and 10 kHz. The value of $\tan\delta$ is lower in the low temperature region as compared to the high-temperature region. In the the high temperature area, tangent loss rises sharply mostly due to high conduction based activity. Tables 1 and 2 basically represents the comparison between the dielectric parameters (permittivity and loss factor) of the prepared composites. In case of BNT- BT-2 there are the presence of two dielectric anomalies (T_d and T_c). Around 200 °C, as represented by T_d (depolarization temperature) shows the transition from ferroelectric to antiferroelectric, whereas around 340 °C (represented by T_c , Curie temperature/ maximum temperature) corresponds to the antiferroelectric to the paraelectric phase transitions. The loss tangent gets enhanced with an increment of the temperature when the dipole movement reaches a maximum value at a certain temperature [18]. It is seen that in case of the prepared composites the expected dielectric anomaly does not lie in the investigated range of temperature due to the causes mentioned above.

Figure 3 shows the frequency dependence of dielectric permittivity and tangent loss (inset) at selected temperature (c) 25 °C and (d) 100 °C. At room temperature, it is seen that

Table 1 Comparison of permittivity and loss for BP-1, BP-2, BP-3 for 1 kHz at 160 °C

Composition	Permittivity	Loss factor
BP-1	42	2.3
BP-2	82	2.4
BP-3	200	2.0

Table 2 Comparison of permittivity and loss for BP-1, BP-2, BP-3 for 10 kHz at 160 °C

Composition	Permittivity	Loss factor
BP-1	27	0.7
BP-2	33	1.1
BP-3	61	1.4

permittivity of the prepared material (BNT-BT/PVDF) is much higher than that of the reported PVDF [14, 20]. It is seen that at 25 °C, with increasing the frequency from 1 kHz to 1 MHz, the dielectric permittivity of prepared composites falls yet it remains above 16 yet even at high frequency. The dielectric permittivity of BP-3 is about 21 which is higher than pure PVDF data reported by Luo et al. [14]. The dielectric loss was high at higher frequency may be due to interfacial polarization, which emerged from the relaxation. In the region of 10 kHz to 100 kHz little variation occurs and further at 1000 kHz, there is occurrence of peak is noted. This is ascribing the glass transition, relaxation of polymer (PVDF) and represents α relaxation [21, 22]. At temperature 100 °C, it is seen that the permittivity value increases at lower frequency where as the curves of all prepared composites coincides at lower frequency. It is observed from the plot that with a rise in the frequency permittivity and loss factor magnitude reduces. At the low frequency various polarizations (i.e., interfacial, dipolar, atomic, ionic) is active leading to high values of permittivity and loss, but at region of higher frequencies these effects of polarization fades. The electronic polarization is dominant in this region of higher frequency. The permittivity value rises similar to the loss factor curve with a rise in the temperature. The interaction between the electron-phonon and thermally activated transport property of the prepared composites may lead to such trend [23]. At higher temperature the charge carriers gain much energy leading to the high value of conductivity in the material resulting to rise the loss factor magnitude. The dielectric constant and loss tangent (inset) at selected temperatures (25 and 100 °C) of PVDF is been presented in Fig. 3e.

Impedance

Complex Impedance spectroscopy (CIS) is regarded as a strong tool to examine the dynamics of mobile and bound charges in the bulk and interfacial areas of any materials. It differentiates the grain, grain boundary and electrode interface contributions in the polarization mechanism. An appearance of successive semicircular arcs in the Z' versus Z'' (Nyquist) plot represents each of these contributions. A Debye type relaxation behavior is suggested if a perfect semicircular arc with center on the real Z' axis is observed in Nyquist Plot. It suggests perfect homogenous material and a

parallel RC circuit acts as an equivalent modeling circuit. In this model, The resistive (Z') and the reactive (Z'') component of the complex impedance can be denoted as: $Z' = \frac{R}{1+(\omega\tau)^2}$ and $Z'' = \frac{-\omega R\tau}{1+(\omega\tau)^2}$, where R being the ac resistance expressed as: $R = \frac{R_{dc}}{\omega C' R_{dc} + 1}$ and $\tau = C'R$; C' and C'' are the real and imaginary components of the capacitance.

From Fig. 4a, b, it is seen at the low frequency range, the value of Z' is higher, and it reduces with increase in the temperature. A negative temperature coefficient of resistance (NTCR) behavior of the material is depicted. In the range of high-frequency, Z' coincides irrespective of the difference in compositions for both temperatures demonstrating the reluctance/inertia of the space charge in following the fast varying electric field. The frequency vs. imaginary part of the complex impedance (Z'') is shown in Fig. 4a, b inset. There is an appearance of characteristic frequency seen to rise with enhancement in temperature, suggesting a temperature

dependent relaxation mechanism. The peaks are prominent at room temperature (25 °C) and the value gradually falls at high temperature (100 °C) in the low frequency region. Such trend may persist because of low temperature immobile species exist, whereas at high temperature there is an activation of defects [24]. This denotes the spreading of the relaxation time with temperature. For BNT-BT-2, the Z' magnitude decreases with increment in temperature at low frequencies which is analogous to semiconductor behavior of material while the rise in the temperature, Z'' reduces showing the presence of relaxation process in the material due to low-temperature immobility of species [18]. The frequency dependent real and imaginary component (inset) of impedance at selected temperatures (25 and 100 °C) of PVDF is been presented in Fig. 4c. Here loss tangent and imaginary part of impedance shows the presence of various relaxation mechanisms with different time constants.

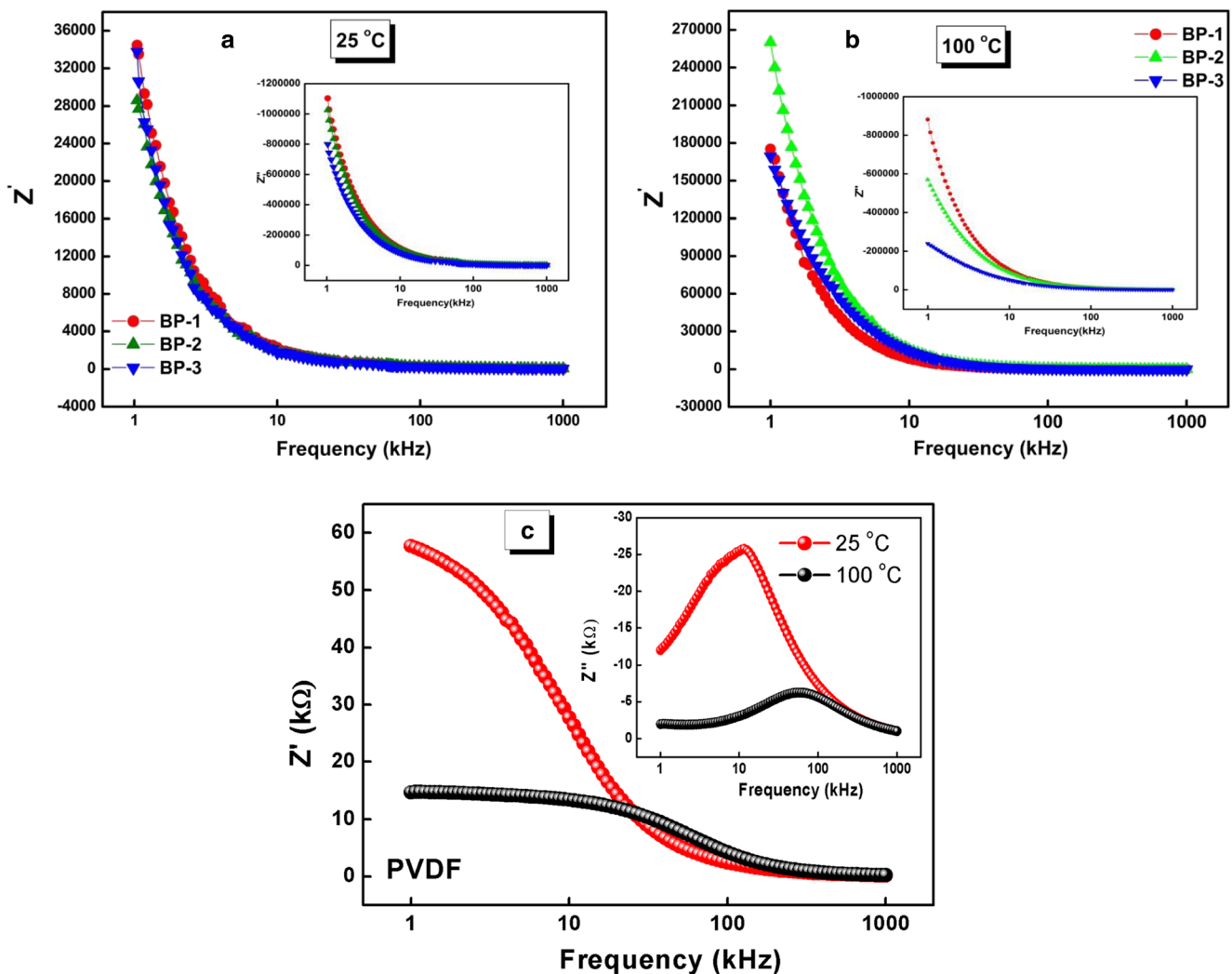


Fig. 4 a, b Frequency dependent real and imaginary (inset) part of impedance at 25 and 100 °C for prepared composites. c Frequency dependent real and imaginary (inset) part of impedance at 25 and 100 °C for pure PVDF

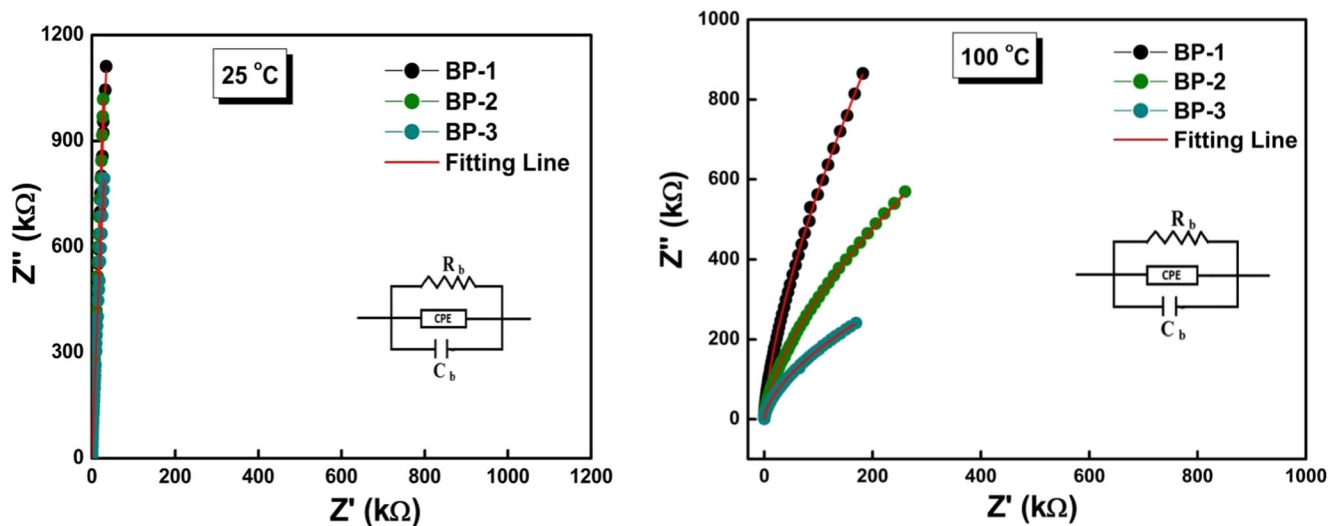


Fig. 5 Nyquist plot at 25 and 100 °C and equivalent circuit model (Inset)

Nyquist plot

Figure 5 presents the relationship between the components of complex impedance Z' (real) and Z'' (imaginary) at different temperature and frequency for the prepared composites. The non-uniform distribution of grains can be identified from the depressed semicircular arc at both 25 and 100 °C. In both the plots, it can be seen that a single depressed semicircular arc with center lying below the real Z' axis depicts non-Debye type of relaxation [25, 26]. This deviation from the ideal Debye mature may be due to the stress-stress phenomena, grain orientation/inhomogeneity and distribution of atomic defects [27]. From the spectrum, it can be identified that there are only contributions of grains. By observing the experimental data, a circuit comprising of the resistor (i.e., the conductive path) and capacitor is proposed. The software package (ZSIMP WIN version 2.0) is used to fit the theoretically calculated data with experimental data for determining the relaxation mechanism type (Debye or non-Debye). The fitted curves for both temperatures (25, 100 °C) is made up of parallel combination of RQC circuit where R = resistance, C = capacitance and Q = constant phase. The value of grain resistance (R) and grain capacitance (C) are calculated from different prepared composites at 25 and 100 °C by using the fitted curve, that provide the contribution to the conductivity and resistivity of the material in Tables 3 and 4. It is seen that with rise in the temperature (25 °C and 100 °C) the grain resistance decreases depicting a NTCR (negative temperature coefficient resistance) behaviour is all the

prepared composites [28, 29]. The relative permittivity is calculated using the formula $\epsilon = Cd/\epsilon_0 A$ where symbols have the usual meaning. The bulk conductivity is evaluated from the formula $\delta_{dc} = 1/R \times d/A$ where R = bulk resistance, d = thickness and A = capacitor area (in m^2). It is noticed there is increase and decrease in the value of grain resistance with rise in temperature so combined NTCR and PCTR behaviour are reported for BNT-BT-2. It is noticed in the reported result for BNT-BT-2 by us, that the semicircle formed is depressed and it deviates from the ideal Debye behaviour [18].

Modulus

Modulus analysis is a tool used to investigate the field and thermal effect on the transport characteristics of ceramic, glass and poly-crystalline sample. In case of the invariable displacement current, the modulus (electrical) is interrelated to the dielectric relaxation behavior [30]. The subsequent relations of the imaginary component (M'') and real component (M') of complex electrical modulus are applied to study our experimental data (with $A = C_0/C$).

$$M' = A \left[\frac{(\omega RC)^2}{1 + (\omega RC)^2} \right] = A \left[\frac{\omega^2 \tau^2}{1 + \omega^2 \tau^2} \right]$$

$$M'' = A \left[\frac{\omega RC}{1 + (\omega RC)^2} \right] = A \left[\frac{\omega \tau}{1 + \omega^2 \tau^2} \right]$$

Table 3 The values of grain resistance (R_g), grain capacitance (C_g) and bulk conductivity of various composites at 25 °C calculated and compared

Composition	Model	R_g (Ω)	C_g (f)	Bulk conductivity	Relative permittivity
BP-1	(RQC)	1.269×10^8	6.381×10^{-15}	8.587×10^{-9}	4.594×10^{15}
BP-2	(RQC)	2.600×10^8	1.579×10^{-19}	3.891×10^{-9}	1.054×10^{15}
BP-3	(RQC)	1.080×10^8	1.490×10^{-19}	8.798×10^{-9}	7.548×10^{14}

Table 4 The values of grain resistance (R_g), grain capacitance (C_g) and bulk conductivity of various composites at 100 °C calculated and compared

Composition	Model	R_g (Ω)	C_g (f)	Bulk conductivity	Relative permittivity
BP-1	(RQC)	1.366×10^9	1.383×10^{-10}	7.9776×10^{-10}	17.029
BP-2	(RQC)	2.032×10^7	1.489×10^{-10}	4.9798×10^{-8}	17.025
BP-3	(RQC)	4.671×10^6	2.257×10^{-10}	2.0343×10^{-7}	24.233

Figure 6a, b presents the frequency variation of the M' (inset) and M'' at some selected temperatures (25, 100 °C) for the prepared composites. The value of M'' rises with the rise in frequency at both the temperature and try to attain a maximum peak which suggests a relaxation phenomenon in the material. There is an asymmetric peak broadening suggests the non-Debye type conduction mechanism in the compound and further there is spread of relaxation with different time constants [31]. It is seen that the M' for temperatures 25, 100 °C increases almost linearly. It is observed that the real

part of the modulus move towards zero at lower frequencies illustrating small or nonexistence of electrode polarization [32] whereas the M' value coincides with the rising frequency with monotonic dispersion may be ascribed to the conduction phenomenon due to the shorter range mobility of charge carriers [33]. For BNT-BT-2, it is observed that in the low frequency region, M' approaches to zero and on increasing the frequency there is a continuous dispersion. It is seen that in case of M'' , there is a asymmetric peak broadening ascribes non-Debye type relaxation that shows the distribution of

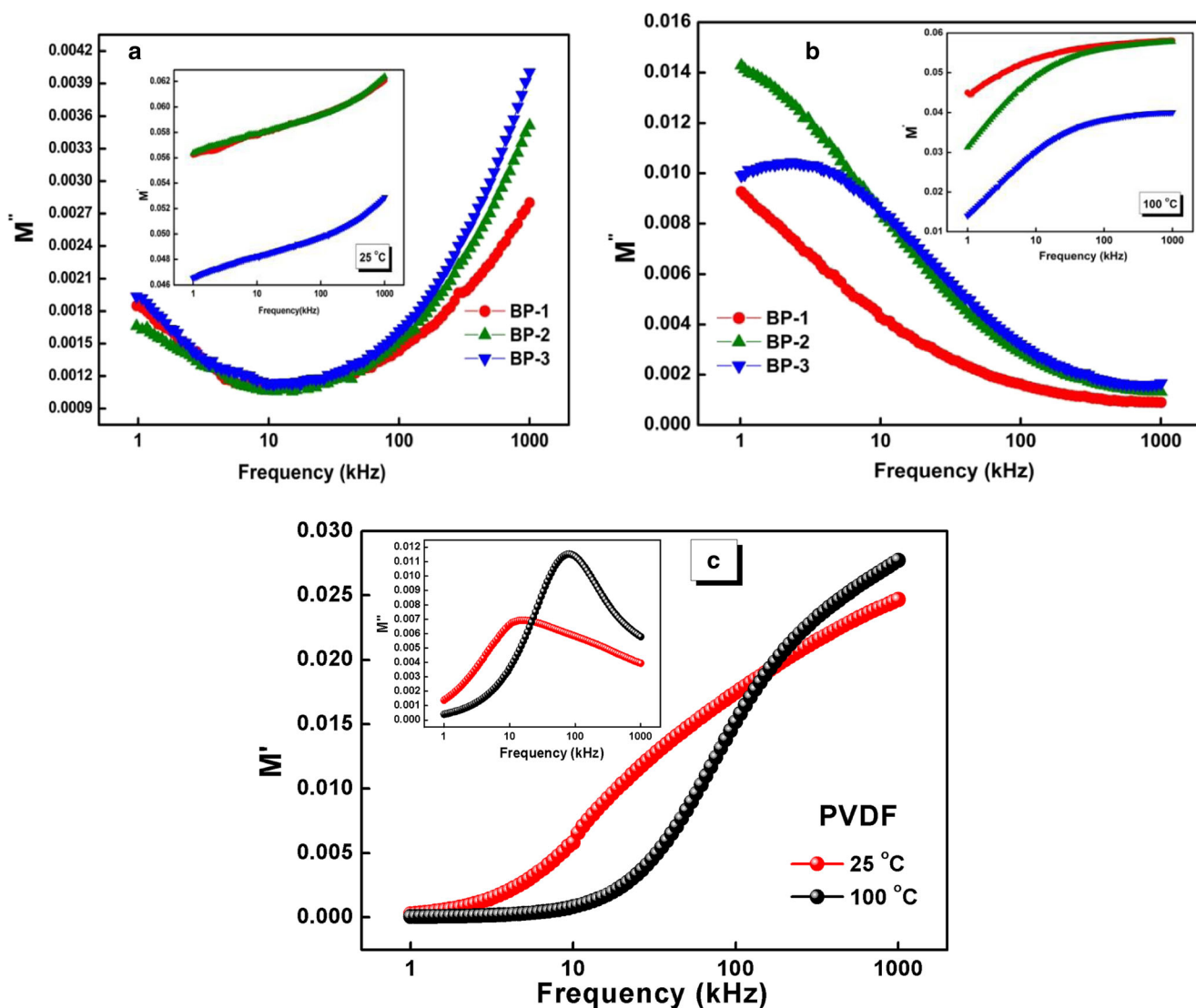


Fig. 6 a, b Frequency dependent real (inset) and imaginary part of modulus at 25 and 100 °C. c Frequency dependent real (inset) and imaginary part of modulus at 25 and 100 °C for pure PVDF

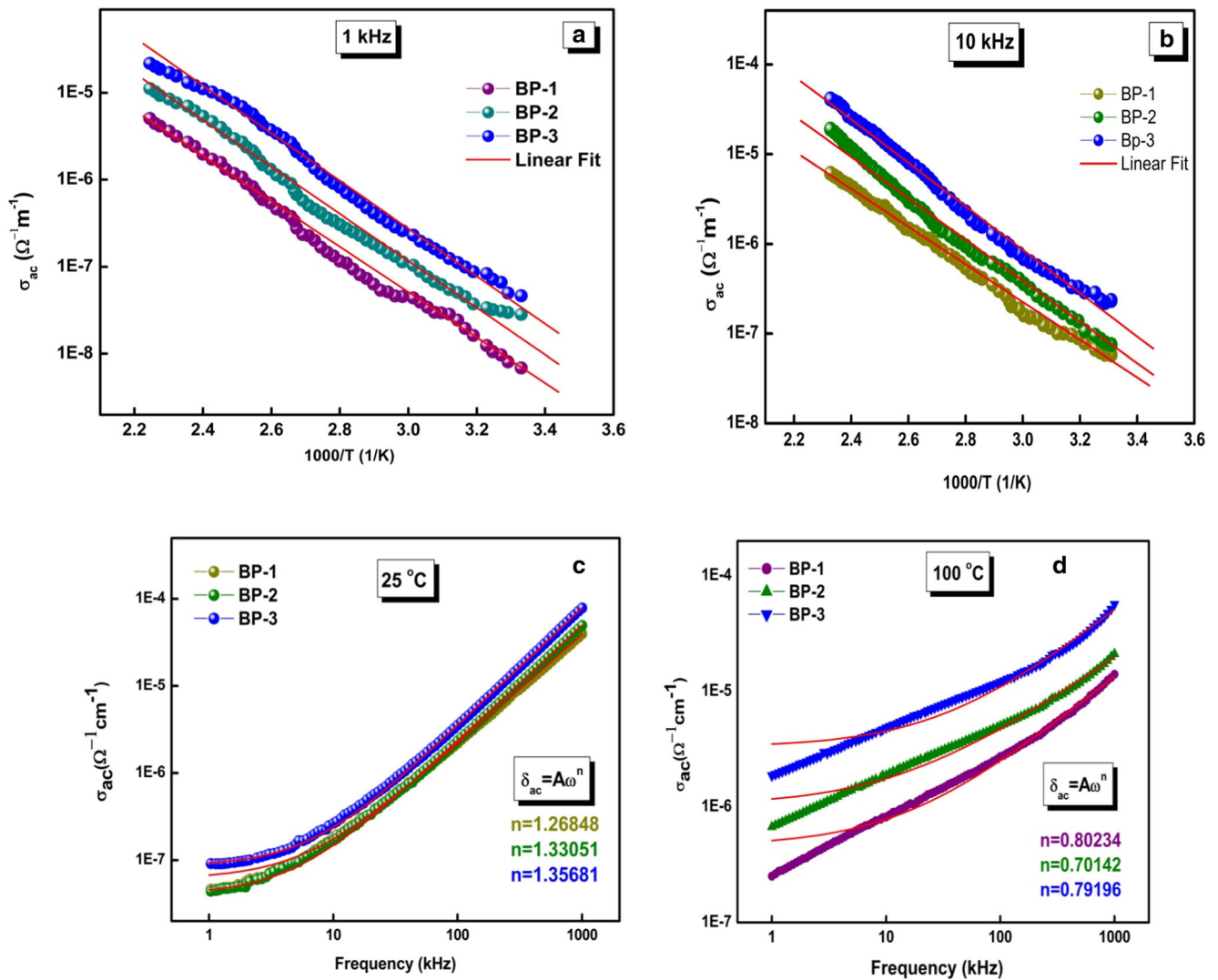


Fig. 7 Temperature dependent AC conductivity at (a) 1 kHz and (b) 10 kHz. Variation of AC conductivity with frequency at (c) 25 °C and (d) 100 °C

relaxation times with various time constant [18]. The frequency dependent real and imaginary (inset) component of modulus at selected temperatures (25 and 100 °C) of PVDF is being presented in Fig. 6c. The imaginary component of modulus of PVDF shows the non Debye type of relaxation process with different time constants.

Conductivity

From Fig. 7a, b it shows the AC conductivity variation with the inverse of absolute temperature at 1 and 10 kHz. This follows the Arrhenius relation; $\sigma_{ac} = \sigma_0 \exp.(-E_a/k_B T)$, where σ_0 symbols represent usual meaning [34]. The activation energy is calculated from the slope of the $\ln\sigma$ versus $1000/T$ plot. At frequency 1 kHz, the activation energy of BP-1, BP-2, BP-3 is found to be 0.0142, 0.0100, 0.0061 where as for frequency 10 kHz, the activation energy of BP-1, BP-2, BP-3 is 0.0153, 0.0115, 0.0072 respectively. The AC conductivities

of the prepared composites exhibit larger value at high temperature than at lower temperature region. When there is a rise in the temperature the polymer chain mobility rises and the fraction of free volume in the prepared composites also enhances. In modified ceramics there is a much more oxygen vacancies. Hence, the free volume fraction of prepared composites leads to the translation motion of the charge carriers and higher activation energy is observed. Defect related to $V_{Bi}^{\bullet\bullet}$ (bismuth) and oxygen vacancies ($V_o^{\bullet\bullet}$) acts as mobile charges and influence the conduction and polarization fatigue [35]. The conductivity data in Fig. 7 are analyzed on the basis of Jonscher power law to reflect on the conduction mechanism. The law basically deals on two well potential models where the localized charge carrier can transit from the initial position to a different site on the application of electric field. The hopping occurs either easily contributing towards dielectric relaxation or difficult to contribute towards conduction. So, there is an interrelation between the conductivity and

dielectric relaxation [36]. The Jonscher power law appears as; $\sigma_{ac} = \sigma_{dc} + A\omega^n$, where 'A' is thermally activated constant determining the polarizability strength and 'n' represents the amount of interaction among mobile ions and lattices [37]. The relation $n > 1$ suggests localized hopping of the entity without leaving the local environment and the relation $n < 1$ suggests translational motion with abrupt hopping. It can be seen in Fig. 7 that the value of n is more than 1 for 25 °C and less than 1 for 100 °C calculated from the non-linear fitting. At 100 °C it is observed that the lower frequency curve for all prepared composites does not fit well with Jonscher power law due to grain boundary blocking effect [29]. For BNT-BT-2, the activation energy is calculated using the Arrhenius relation from slope was seen to enhance from 0.55 eV (1 kHz) to 0.68 eV (100 kHz) in the high-temperature region [18].

Conclusion

BNBT/PVDF composite flexible films were prepared by a solvent casting route. A high dielectric permittivity and low loss factor were obtained from the prepared composites. The SEM results depict a close and high density packing of grains. The powder was homogeneously distributed throughout the matrix. The value of permittivity enhanced with adding of ceramic material into the matrix. The conduction mechanism and dielectric relaxation were investigated using impedance and modulus spectroscopy. The activation energy for all test composites was obtained from temperature dependent AC conductivity plot. The analyses of the conductivity data using Jonscher's power law indicate that the conduction mechanism is based on the translational motion of the charge carriers with hopping. The above experimental results suggests high flexibility, cheap processing, high permittivity with low loss factor making it a possible base for embedded capacitor and devices. Further, as a base for device engineering, the BP-3 may be preferred due to its excellent properties like high dielectric constant and low loss.

Acknowledgements The authors like to express their sincere gratitude to Dr. Kalyani Mohanta, Indian Institute of Technology, BHU, Varanasi for her kind help in carrying out SEM investigation.

References

- Haertling GH (1999) Ferroelectric ceramics: history and technology. *J Am Ceram Soc* 82:797–818
- Lovinger AJ (1983) Ferroelectric Polymers. *Science* 220:1115–1121
- Pan J, Li K, Li J, Hsu T, Wang Q (2009). *Appl Phys Lett* 95
- Saravanakumar B, Mohan R, Thiyagarajan K, Kim SJ (2013) Fabrication of a ZnO nanogenerator for eco-friendly biomechanical energy harvesting. *RSC Adv* 3:16646–16656
- Hong CC, Huang SY, Shieh J, Chen SH (2012) Enhanced Piezoelectricity of Nanoimprinted Sub-20 nm Poly(vinylidene fluoride-trifluoroethylene) Copolymer Nanograss. *Macromolecules* 45:1580–1586
- Seymour RB, Kauffman GB (1990). *J Chem Educ* 67, 763
- Seol ML, Woo J-H, Lee D-I, Im H, Hur J, Choi YK (2014). *Small* 10:103887–103894
- da Costa GCC, Simoes AZ, Ries A, Foschini CR, Zaghete MA, Varela JA (2004). *Mater Lett* 21, 414
- Nan CW, Weng GJ (2000) Influence of polarization orientation on the effective properties of piezoelectric composites. *J Appl Phys* 88:416–423
- Chu B, Zhou X, Ren K, Neese B, Lin M, Wang Q, Bauer F, Zhang QM (2006) A Dielectric Polymer with High Electric Energy Density and Fast Discharge Speed. *Science* 313:334–336
- Kobayashi Y, Tanase T, Tabata T, Miwa T, Konno M (2008) Fabrication and dielectric properties of the BaTiO₃-polymer nano-composite thin films. *J Eur Ceram Soc* 28:117–122
- Song Y, Shen Y, Hu P, Lin Y, Li M, Nan CW (2012) Significant enhancement in energy density of polymer composites induced by dopamine-modified Ba_{0.6}Sr_{0.4}TiO₃nanofibers. *Appl Phys Lett* 101:152904
- Thomas P, Satapathy S, Dwarakanath K, Varma KBR (2010) Dielectric properties of poly(vinylidene fluoride)/CaCu₃Ti₄O₁₂ nanocrystal composite thick films. *Express Polym Lett* 4:632–643
- Luo B, Wang X, Wang Y, Li L (2014) Fabrication, characterization, properties and theoretical analysis of ceramic/PVDF composite flexible films with high dielectric constant and low dielectric loss. *J Mater Chem A* 2:510–519
- Tiwari V, Srivastava G (2015) Structural, dielectric and piezoelectric properties of 0–3 PZT/PVDF composites. *Ceram Int* 41:8008–8013
- Deepa KS, Shaiju P, Sebastian MT, Bhoje Gowd E, James J (2014). *PhysChemChemPhys* 16:17008–17017
- Elashmawi IS, Abdelrazek EM, Ragab HM, Hakeem NA (2010) Structural, optical and dielectric behavior of PVDF films filled with different concentrations of iodine. *Physica B* 405:94–98
- Hajra S, Sahoo S, De M, Rout PK, Tewari HS, Choudhary RNP (2018). *J Mater Sci Mater Electron* 29:1463
- Sailaja JM, Murali N, KV Babu VV (2017) *Journal of Asian ceramic. society* 5:18–30
- Dash S, Choudhary RNP, Goswami MN (2017) Enhanced dielectric and ferroelectric properties of PVDF-BiFeO₃ composites in 0–3 connectivity. *J Alloys Compd* 715:29–36
- Yu K, Wang H, Zhou Y, Bai Y, Niu Y (2013). *J Appl Phys* 113
- Chanmal CV, Jog JP (2008) Dielectric relaxations in PVDF/BaTiO₃ nanocomposites. *Express Polym Lett* 2:294–301
- Parida BN, Das PR, Padhee R, Choudhary RNP (2012) Phase transition and conduction mechanism of rare earth based tungsten-bronze compounds. *J Alloy Compd* 540:267–274
- Koop CG (1951) On the Dispersion of Resistivity and Dielectric Constant of Some Semiconductors at Audiofrequencies. *Phys Rev* 83:121–124
- Gupta P, Padhee R, Mahapatra PK, Choudhary RNP (2017). *J Mater Sci Mater Electron* 28:17344–17353
- Wang T, Hu J, Yang H, Jin L, Wei X, Li C, Yan F, Lin Y (2017). *J Appl Phys* 121
- Barick BK, Choudhary RNP, Pradhan DK (2013) Dielectric and impedance spectroscopy of zirconium modified (Na_{0.5}Bi_{0.5})TiO₃ ceramics. *Ceram Int* 39:5695–5704
- Dash U, Sahoo S, Chaudhuri P, Parashar SKS, Parashar K (2014). *J Adv Ceram* 3:89–97
- Parida K, Dehury SK, Choudhary RNP (2017) Electrical, optical and magneto-electric characteristics of BiBaFeCeO₆ electronic system. *Mater Sci Eng B* 225:173–181

30. Richert R, Wagner H (1998) The dielectric modulus: relaxation versus retardation. *Solid State Ionics* 105:167–173
31. Macdonald JR (1984) Note on the parameterization of the constant-phase admittance element. *Solid State Ionics* 13: 147–149
32. Parida BN, Padhee R, Suara D, Mishra A, Choudhary RNP (2016). *J Mater Sci Mater Electron* 27:9015–9021
33. N. Panda, B.N. Parida, R. Padhee, R.N.P. Choudhary, .J. Mater. Sci: Mater Electron, 26 (2015) 3797–3804
34. Purohit V, Padhee R, Choudhary RNP (2018) Dielectric and impedance spectroscopy of Bi(Ca 0.5 Ti 0.5)O 3 ceramic. *Ceram Int* 44:3993–3999
35. Kröger FA, Vink HJ (1956). *Solid State Phys* 3:307–435
36. Behera B, Nayak P, Choudhary RNP (2008) Structural and impedance properties of KBa₂V₅O₁₅ ceramics. *Mater Res Bull* 43:401–410
37. De M, Hajra S, Tiwari R, Sahoo S, Choudhary RNP, Tewari HS (2018) Structural, dielectric and electrical characteristics of BiFeO₃-NaNbO₃ solid solutions. *Ceram Int* 44:11792–11797